Seismic performance curve of lightly reinforced shear wall for use in fragility calculation

JIAYU YAN[1]

[1] *Chinergy Co. Ltd, Beijing, China, 100193, jyyan@chinergy.com.cn*

ABSTRACT

Seismic safety of structures is a critical issue for nuclear power plants and seismic fragility evaluation has been a vital procedure for seismic probabilistic safety assessment. In the structural system of nuclear power plants, shear walls are the primary seismic-resistant components and generally designed with low rises. Herein, the seismic performance of a low-rise lightly reinforced shear wall in the structure of high-temperature reactors was investigated. A time-history analysis of a detailed finite element model was employed to extract the seismic demand of the shear wall. Then, its seismic force-shear strength curve was plotted through shear strength equations for three failure modes and with reference to this curve, the failure mode of a specific shear wall can be predicted. Subsequently, a new method to calculate the strength factor of the shear wall was proposed based on the plotted curve and data points of simulated seismic in-plane shear and axial force. Compared with the conventional iterative method, the proposed method requires less computational effort. Different load combinations of seismic in-plane shear and axial force were compared in terms of the strength factor and it was found that there was conservatism in the design load combination of maximum shear-maximum tensile axial force, whereas for use in fragility calculation, a logarithmic standard deviation for seismic shear-axial force combination randomness should be considered to yield a more precise risk assessment of structures for seismic probabilistic safety assessment.

Keywords: Seismic performance, Fragility, Shear wall

I. INTRODUCTION

Performance-based methodologies has emerged as a prospective approach for structure, system and component (SSC) design and risk assessment of nuclear power plants (NPPs). Particularly for seismic performance, it serves as a decisive factor for the design of the majority of SSCs. On this topic, intensive researches has been conducted and the method of fragility evaluation has gradually gained recognition to quantify the seismic performance of SSCs. The fragility evaluation also serves as a critical procedure in seismic probabilistic safety assessment (SPSA), requiring complex analysis and computations. According to EPRI 3002012994 [1], seismic fragility is calculated as the ratio of capacity over demand (the capacity factor, F_c) multiplied by response factors and the ground motion parameter. To a significant extent, the capacity factor represents the seismic performance and provide a prediction for failure mode of SSCs under seismic events.

Compared to conventional pressurized water reactors (PWRs), the structural design of high-temperature reactors (HTRs) in Weihai, Shandong, China is more flexible and smaller in mass. As main lateral load-carrying structural components, shear walls were designed with lightly reinforcements (steel reinforcement ratios less than 0.01), which raised concerns about their seismic performance. Therefore, in this study, the seismic performance of lightly reinforced shear walls was evaluated based on the fragility method. A time-history analysis of structures of HTRs was conducted to obtain the seismic responses of shear walls. Three failure modes (diagonal shear cracking, flexure and shear friction) were considered to calculate the strength factor of a typical shear wall and its lateral load-carrying performance curve was plotted. Through the performance curve, the seismic capacity of a specific shear wall can be quantified and a novel method to calculate the capacity factor was proposed accordingly. Finally, different combinations of seismic-induced shear and axial force were discussed to reduce the conservatism for SPSA.

II. TIME-HISTORY ANALYSIS

II.A. Ground Motion

The reference earthquake used in SPSA of HTRs was based on the site-specific mean uniform hazard response spectrum (UHRS) conditioned on the 1E-6 annual exceedance frequency. The horizontal UHRS was developed by a probabilistic

seismic hazard assessment (PSHA), and had peak ground acceleration (PGA) of 0.347g. The vertical UHRS was derived by multiplying horizontal UHRS by the V/H ratio of 2/3, resulting in 0.231g.

For the time-history analysis, modified recorded earthquake ground motion time histories were generated targeting the 5% damped UHRS. One set of three-component acceleration time series employed in this study has been selected as No.2625 from the Next Generation Attenuation (NGA) Acceleration Record Database. Fig.1 presents the modified acceleration time series of ground motion. With reference to ASCE SEI4-16 [2], three orthogonal components are statistically independent with a time increment of 0.010s and a total duration of 25s, which can be input to the numerical model of the structure simultaneously.

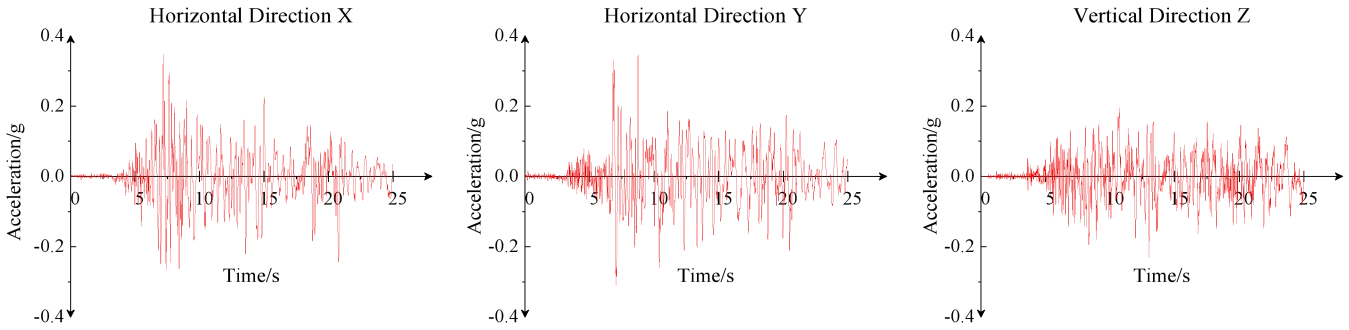

FIGURE 1. Acceleration time series of ground motion.

II.B. Finite Element Model

The time-history analysis of structures of HTR was performed based on a detailed finite element modal, as shown in Fig. 2. The mass of the model included the dead load, 25% of the specified design live load and snow load on the roof. The main structure was constructed with Grade 35 concrete, and curing age factor of 1.2 was considered in its material properties. Proportional damping as 7% damping ratio was incorporated into the model. The structural components, shear wall and diaphragms, were modeled as shell elements while raft foundation and containment were simulated as solid elements. Mesh sizes were controlled within 1m. The soil-structure interaction effect was not considered since the structures were supported by a rock foundation (shear wave velocity greater than 2400m/s).

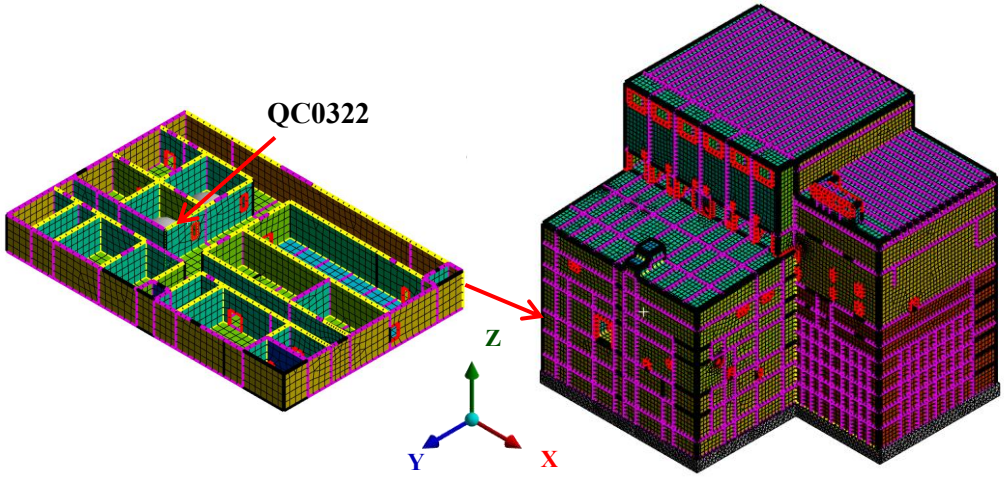

FIGURE 2. Finite element modal of HTR structures and location of shear wall QC0322.

The acceleration time series of ground motion were applied into the model to calculate the seismic-induced forces,then a gravitational acceleration was exerted on the model separately to obtain the forces under the operating condition. After linear time-history analysis, the time-varying internal forces in specific structural components can be extracted from the model and for the shear wall, in-plane shear force and axial force were primary outputs for subsequent analysis.

III. SEISMIC PERFORMANCE CURVE

III.A. Failure mode

Seismic capacity of shear walls is primarily assessed based on its in-plane lateral force resistance. In determining seismic capacity, three failure modes are required to be investigated [1]: diagonal shear cracking, flexure and shear friction. In this study, the strength equations associated with each failure mode are chosen as follows.

III.A.1. Diagonal shear cracking

The Barda equation is a widely adopted approach to evaluating the median shear capacity of low-rise shear walls in NPPs, as provided in EPRI 3002012994 [1]:

$$V_{um} = v_{um} * d_m * t_n \quad (1)$$

Where

$$v_{um} = v_{cm} + v_{sm} \quad (2)$$

$$v_{cm} = 8.3 * \sqrt{f'_{cm}} - 3.4 * \sqrt{f'_{cm}} * (\frac{h_w}{l_w} - 0.5) + \frac{N_a}{4 * l_w * t_n} \quad (3)$$

$$v_{sm} = \min(\rho_{se} * f_{ym}, 600) \quad (4)$$

$$\rho_{se} = A_1 * \rho_v + A_2 * \rho_h \quad (5)$$

$$d_m \approx 0.6 * l_w \quad (6)$$

And v_{um} is median ultimate shear strength, psi; v_{cm} is median strength contribution from concrete, psi; v_{sm} is median strength contribution from steel reinforcement, psi; f'_{cm} is median concrete compressive strength, psi; h_w is height of wall, in; l_w is length of wall, in; t_n is thickness of wall, in; N_a is axial force in wall, lb, for which negative values signify tension while positive values for compression; $d_m$is distance from extreme compression fiber to center of force of all reinforcement in tension, in; f_{ym} is median steel yield strength, psi; ρ_{se} is effective steel reinforcement ratio; ρ_v is vertical steel reinforcement ratio; ρ_h is horizontal steel reinforcement ratio. A_1, A_2 constants given as follows:

For $\frac{h_w}{l_w} \leq 0.5$,	$A_1=1$	$A_2=0$	
For $0.5 \leq \frac{h_w}{l_w} \leq 1.5$,	$A_1=-(\frac{h_w}{l_w}) + 1.5$	$A_2=(\frac{h_w}{l_w}) - 0.5$	(7)
For $1.5 \leq \frac{h_w}{l_w}$	$A_1=0$	$A_2=1$	

III.A.2. Flexure

The moment capacity of a shear wall is determined by the strength equation provided by Kennedy, et al. (Report No. 1643.1) [3], as follows:

$$M_{cap,m} = (A_{s_v m} * f_{ym} + N_a) * (\frac{l_w}{2} - \frac{a_m}{2}) \quad (8)$$

Where

$$a_m = \frac{A_{s_v m} * f_{ym} + N_a}{0.85 * f'_{cm} * t_n} \quad (9)$$

$$A_{s_v m} = \rho_v * t_n * l_w \quad (10)$$

And $M_{cap,m}$ is median moment capacity, in-lb; a_m is half the distance from compression face to the point of reinforcement at yield, in; $A_{s_v m}$ is median steel reinforcement area at yield,sq in.

It should be noticed that assuming that the the inflection point is at the midpoint of the wall height, the equivalent shear capacity for a wall section can be obtained by dividing the moment capacity by half the wall height, which can be expressed as:

$$V_{cap,m} = \frac{M_{cap,m}}{h_w/2} \quad (11)$$

III.A.3. Shear friction

Reference [5] modified the shear-friction strength equation in ACI 349 [6]. And when shear-friction reinforcement is perpendicular to the shear plane, the equation is expressed as:

$$V_{nm} = \mu(A_{s_v m} f_{vfs} + \mathrm{Max}(0, N_a)) \leq \min(0.2 f'_{cm} A_C, 1000 A_C) \quad (12)$$

Where

$$f_{vfs} = \min(E_y * \varepsilon_{se}, f_{ym}) \quad (13)$$

$$A_C = t_n * l_w \quad (14)$$

And V_{nm} is median shear-friction strength, lb; A_C is area of concrete section resisting shear transfer, sq in; A_{vf} is area of vertical reinforcement to resist shear, sq in; f_{vfs} is effective stress of vertical reinforcement, psi; E_y is modulus of elasticity of steel reinforcement, psi; ε_{se} is effective strain of vertical reinforcement.

III.B. Seismic force-shear strength curve

The seismic capacity of shear walls can be evaluated based on the aforementioned shear strength equations. For a specific shear wall of structure, its seismic force-shear strength curve can be drawn accordingly, since the seismic forces act on the axial force of the wall, thereby influencing its shear strength. This study selected a lightly reinforced shear wall within structure of HTR for analysis, with its location shown in Fig. 2 and required key information presented in Table 1. Through the linear time-history analysis, the time-varying in-plane shear force and axial force under seismic action can be extracted from the finite element model. Besides, the axial force under normal operation N_{DL} was output as 871970 lb.

TABLE 1. Parameters of Shear Wall QC0322 .

Parameter	Value
Height h_w (in)	165
Length l_w (in)	295
Thickness t_n (in)	16
Vertical steel reinforcement ratio ρ_v	0.00636
Horizontal steel reinforcement ratio ρ_h	0.00636
Modulus of elasticity of steel reinforcement E_y (psi)	29000000
Median steel yield strength f_{ym} (psi)	66807
Median concrete compressive strength f'_{cm} (psi)	6340
Coefficient of friction μ	0.6

It can be observed from Eq.(3), Eq.(8) and Eq.(11), Eq.(12) that the seismic shear strength of the shear wall is related to the axial force it experiences and based on the above information provided in Table 1, the seismic performance curves as a function of the seismic axial force are plotted in Fig. 3 for the shear wall QC0322, while the seismic-induced in-plane shear force and axial force are combined as data points and also marked in the Fig. 3. As can be seen from the comparison of the three curves, the green curve, representing the shear friction strength of the shear wall QC0322, remains below the other two curves when the seismic axial force ranges from -2000 kip to 2000 kip. In other words, compared to diagonal shear cracking and flexure failure, the shear wall QC0322 tends to fail in the form of shear friction under the reference earthquake. For the earthquake scenario with 1E-6 annual exceedance frequency, the shear wall QC0322 will retain its lateral load-carrying capacity, as the numerical data points fall within the failure mode envelope. Nevertheless, for risk quantitative analysis, the capacity factor under the 1E-6 annual exceedance probability earthquake is required for the shear wall, and for non-ductile failure modes like shear friction, the inelastic energy absorption factor F_μ should be excluded, therefore the capacity factor F_c equals the strength factor F_s and can be calculated as [1]:

$$F_c = F_s = \frac{C - D_{NS}}{D_S + \Delta C_S} \tag{15}$$

Where C is elastic capacity of the seismic failure mode; D_S is elastic seismic demand; D_{NS} is non-seismic demand; ΔC_S is reduction in capacity due to concurrent seismic loading.

Based on the definition, the value of F_s can be interpreted geometrically as the distance d_0 to the distance d_1, as illustrated in Fig. 3. d_0 equals to the distance from data point to the origin, and d_1 equals to the distance between the intersection point and the origin. The intersection point is where the line passing through the selected data point and the origin intersects the nearest shear strength curve, and the selected data point should be the one closest to the shear strength envelope.

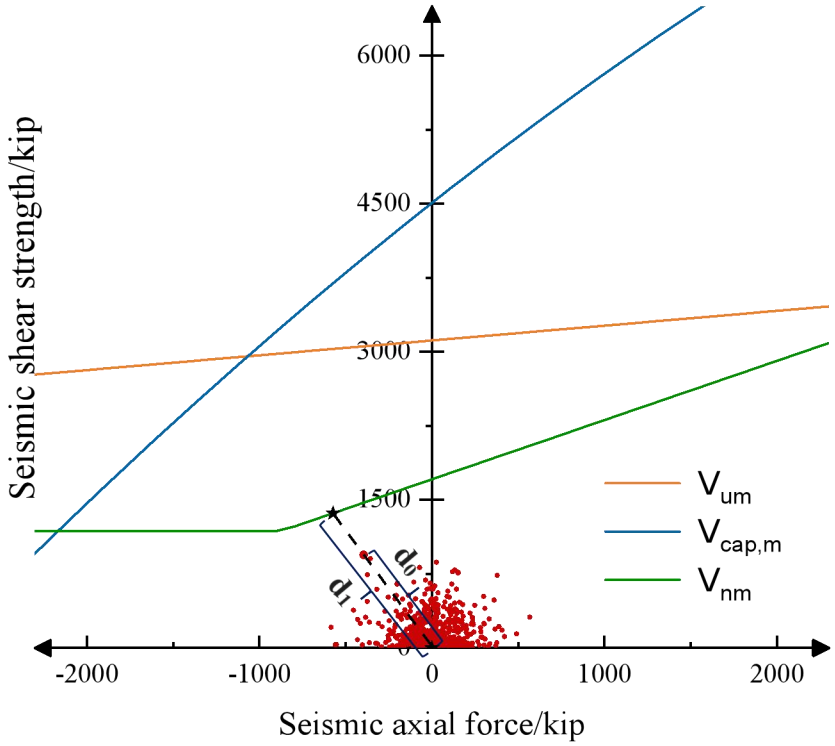

FIGURE 3. Seismic force-shear strength curve of shear wall QC0322.

By this intersection ratio method, F_s of shear wall QC0322 is computed as 1.448 when data point is selected when the maximum shear force occurred. To verify this, the iterative method used in EPRI 3002012994 [1] is also used to calculate the F_s, as listed in Table 2. The F_s is iteratively calculated starting from 2.000 to 1.448 when the error reaches 0. By contrast, the solving process by the intersection ratio method is also illustrated in Table 2. This method mainly involves the calculation of the intersection point (x_1,y_1) , which depends on the selected data point (x_0,y_0) and its nearest shear strength function curve. Once the coordinates of these two points are determined, the values of F_s can be obtained by Eq. 16 as：

$$F_S = \frac{d_1}{d_0} = \frac{\sqrt{x_1^2 + y_1^2}}{\sqrt{x_0^2 + y_0^2}} \tag{16}$$

TABLE 2. Comparsion of solving processes between intersection ratio method and iterative method

Intersection ratio method		Iterative method			
Coordinates of the intersection point (x_1, y_1)	(-573, 1365)	Fs	**2.000**	**1.500**	**1.448**
Coordinates of the data point (x_0, y_0)	(-396, 943)	Na (kip)	81	279	299
d_1	1481	V_{um} (kip)	2996	3026	3029
d_0	1023	$V_{cap,m}$ (kip)	3372	3665	3695
d_1/d_0	1.448	V_{nm} (kip)	1234	1353	1365
Fs	**1.448**	Fs*V_{eq}	1886	1415	1365
		Error	652	62	0

However, the principle for selecting the data point deserves further exploration, which regards how to determine the combination of seismic in-plane shear and axial force. Herein, four different combinations are selected to calculate the F_s, including maximum shear-maximum tensile axial force, maximum shear-corresponding axial force, maximum tensile axial force-corresponding shear and maximum compressive axial force-maximum shear. The results are compared in Table 3. As expected, the smallest F_s corresponds to the combination of maximum shear-maximum tensile axial force, which is considered as the governing load combination for design. However, such combination may exhibit conservatism for SPSA. Since the reaction forces in time-history analysis are time-dependent, the load combinations of maximum shear-corresponding axial force and maximum tensile axial force-corresponding shear are more accurate to calculate the capacity factor, otherwise, logarithmic standard deviation for seismic shear-axial force combination randomness should be accounted during the fragility evaluation.

TABLE 3. Comparison of strength factor between different load combinations.

Load combination	Strength factor
Maximum shear-Maximum tensile axial force	1.321
Maximum shear-Corresponding axial force	1.448
Maximum tensile axial force-Corresponding shear	3.053
Maximum compressive axial force-Maximum shear	2.835

IV. CONCLUSIONS

This paper presents the seismic performance assessment of a lightly reinforced shear wall in the structure of HTR. The seismic demand and capacity of the shear wall were obtained from the time-history analysis and shear strength equations, respectively. The seismic force-shear strength curve was then plotted to compare the shear strength associated with three different failure modes, and by leveraging the curve, an intersection ratio method was proposed to determine the strength factor. Furthermore, the combination methods of seismic in-plane shear and axial force were compared.

For the case of lightly reinforced shear wall studies in this paper, the seismic force-shear strength curve indicates that its shear-friction strength is relatively weak compared to shear and flexural strength under the lateral loading. The critical load combination is identified as maximum shear-maximum tensile axial force for design, while for SPSA, the combinations of maximum shear force-corresponding axial force and maximum tensile axial force-corresponding shear provide a more accurate basis for fragility evaluation.

REFERENCES

[1] Electric Power Research Institute, *Seismic Fragility and Seismic Margin Guidance for Seismic Probabilistic Risk Assessments*, EPRI 3002012994, Palo Alto, CA (2018).

[2] American Society of Civil Engineers, *Seismic Analysis of Safety Related Nuclear Structures and Commentary*, ASCE/SEI Standard 4-16, Reston, VA (2017).
[3] Pacific Gas & Electric Company, *Probabilistic Evaluation of the Diablo Canyon Turbine Building Seismic Capacity Using Nonlinear Time History Analyses,* 1643.1(1998).
[4] American Society of Civil Engineers, *Seismic Design Criteria for Structures, Systems and Components in Nuclear Facilities*, ASCE/SEI Standard 43-05, Reston, VA (2005).
[5] Baek, Jang-Woon & Kim, Sung-Hyun & Park, Hong-Gun & Lee, Byung-Soo. "Shear-Friction Strength of Low-Rise Walls with 600 MPa (87 ksi) Reinforcing Bars", *ACI Structural Journal* 117(1), 117-S14 (2020).
[6] American Concrete Institute, *Code Requirements for Nuclear Safety-Related Concrete Structures and Commentary,* ACI 349-13, Farmington Hills, MI (2013).